A PRELIMINARY ANALYSIS OF FORWARD-SCATTER SIGNALS FROM SHOWERS

by

A. S. DENNIS AND F. G. FERNALD

ABSTRACT

32099

Simultaneous measurements of forward scatter by isolated showers at 4.86 and 9.10 Gc, made by the Central Radio Propagation Laboratory in Colorado, are analyzed with the aid of time-lapse photographic records from a weather radar. The computed scattering cross sections agree with those found by workers in the field of radar meteorology. Comparison of the received power at 4.86 Gc and 9.10 Gc provides definite evidence of non-Rayleigh scattering at 9.10 Gc, particularly near shower cores at altitudes above the freezing level. On the basis of Mie scattering theory, the particles producing the most marked deviations from Rayleigh scattering are tentatively identified as dry hailstones some 1.5 cm in diameter.

Author

NOTICE

The signal levels observed during these tests are not in themselves meaningful measures of the probability of interference due to this mode of propagation. They must be combined with data on occurrence of rain and hail as a function of time, place, and season, and with data on the statistical probability of illuminating a scattering volume from a communications satellite earth station-- or a radio relay station. Work along these lines is planned in 1964, as well as additional measurements of scattering from rain, hail, and wet snow.

October 1963

Research Memorandum 5

A PRELIMINARY ANALYSIS OF FORWARD-SCATTER SIGNALS FROM SHOWERS

Prepared for:

National Aeronautics and Space Administration
Washington, D.C.

SRI Project No. 3773

Contract NASr-49(02)

Submitted by:

A. S. Dennis, Physicist
Aerophysics Laboratory

F. C. Fernald, Research Meteorologist
Aerophysics Laboratory

[redacted]

CONTENTS

ABSTRACT ii

LIST OF ILLUSTRATIONS AND TABLE iv

I INTRODUCTION AND CONCLUSIONS 1

II GEOMETRY OF EXPERIMENT 4

III ANALYSIS OF DATA 7

A. General 7

B. A Situation in Detail 8

C. Calculations of Scattering Cross Sections 10

D. Evidence of Mie Scattering 11

ACKNOWLEDGMENTS 18

REFERENCES 19

ILLUSTRATIONS

Fig. 1 Map Showing Propagation Path 2

Fig. 2 Shower Locations and Received Power as a Function of Receiver Bearing, 1510 MST, 27 June 1963 9

Fig. 3 Integral of Reflectivity Along Shower Diameter as a Function of Shower Size 12

Fig. 4 Ratio of Observed Scattering Cross Section at 9.1 Gc to That at 4.86 Gc, 1607-1619 MST, 27 June 1963 14

Fig. 5 Measured Values of $\eta_c L$, 1607-1619 MST, 27 June 1963 15

Fig. 6 Ratio of Actual Attenuation (by Scattering and Absorption) to That Given by the Rayleigh Approximation, for Water at 18°C 16

TABLE

Table I Equipment Characteristics, CRPL Scatter Experiment. 5

I INTRODUCTION AND CONCLUSIONS

In an earlier memorandum prepared under the present contract,[1*] it was pointed out that precipitation scatter signals constitute a potential source of interference at the ground terminals of a communication satellite system. An experiment to measure forward scattering[†] by rain at 9.05 Gc, carried out by Stanford Research Institute in California early in 1962, yielded results compatible with the assumption of Rayleigh scattering by raindrops conforming to previously observed drop-size distributions.[2] Doherty and Stone had previously reported similar results at 2.72 Gc for a 90-mile path in eastern Canada.[3] On the basis of these experiments, one can estimate interference levels at satellite terminals in continuous-rain situations as a function of rainfall rate with a fair degree of accuracy.

In order to obtain data useful in predicting interference levels due to showers and thunderstorms, the Central Radio Propagation Laboratory of the National Bureau of Standards is conducting a program to measure precipitation scatter in northeastern Colorado, under a contract with the National Aeronautics and Space Administration. In particular, the program is intended to measure scattering by storms producing hail, as Mie scattering theory indicates very large forward-scatter cross sections for hailstones.[4] Measurements are being made at 4.86 Gc (*C* band) and at 9.10 Gc (*X* band), with the transmitters at Akron, Colorado, and the receivers 170 km away at Table Mesa (Fig. 1). In this work, the Central Radio Propagation Laboratory maintains close cooperation with Colorado State University personnel who are studying hailstorms in the same general area. Data provided to the Laboratory by Colorado State University include records from a weather radar set operated at New Raymer (Fig. 1) by Atmospherics, Inc., as part of the University's program.

---

* References are listed at the end of the report.

† We shall use this term for scattering in all directions *other* than directly back to the transmitter.

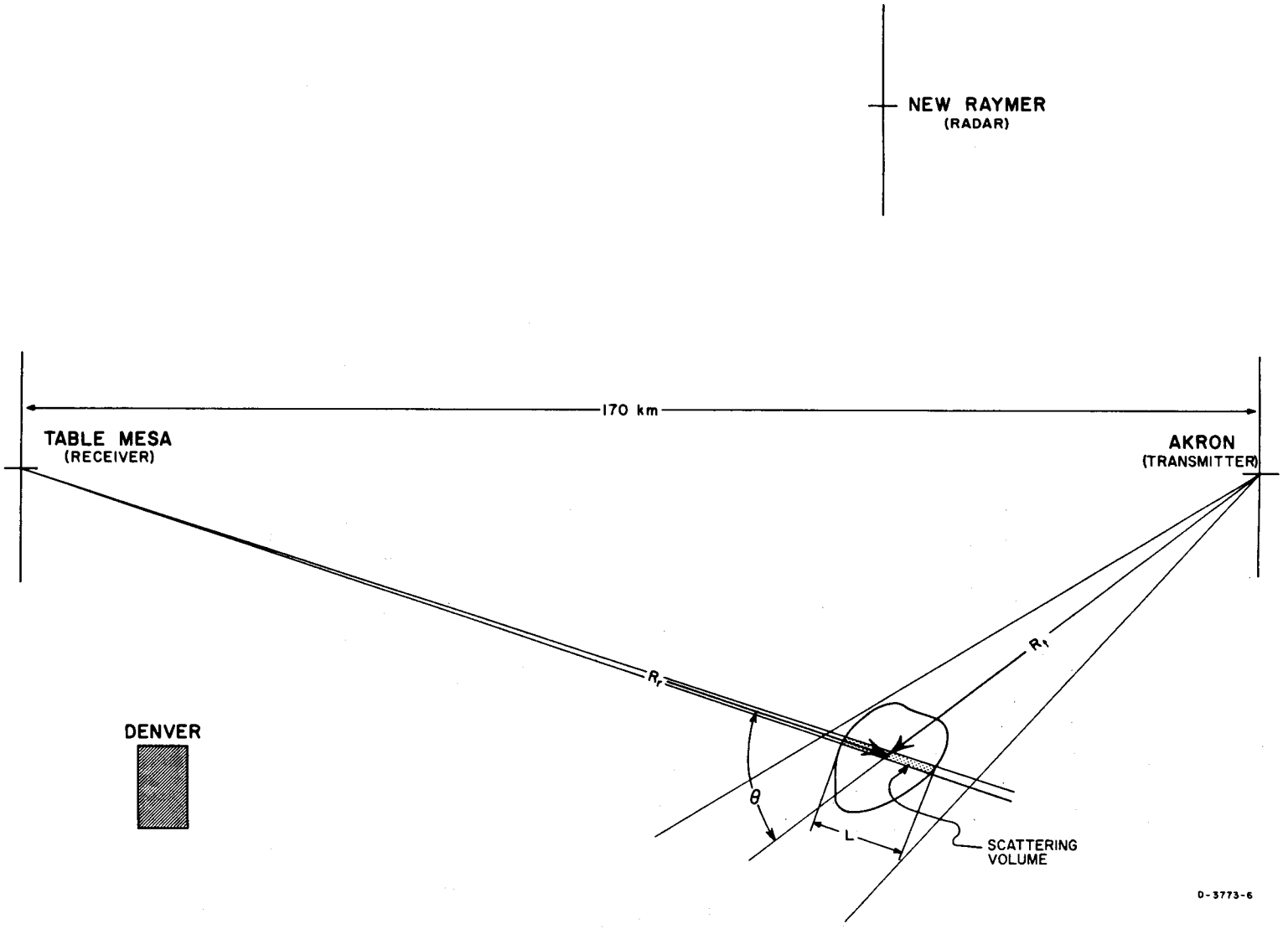

FIG. 1 MAP SHOWING PROPAGATION PATH

This research memorandum contains a preliminary analysis, performed by Stanford Research Institute at the request of the National Aeronautics and Space Administration, of some of the precipitation-scatter data recorded by Central Radio Propagation Laboratory. The scatter signals were recorded simultaneously on magnetic tape and on a Sanborn recorder; duplicate recordings from the Sanborn machine were used in the present work. Time-lapse motion pictures of the New Raymer weather radar screen, provided by Atmospherics, Inc., and Colorado State University, proved indispensable in the analysis of the Sanborn charts.

Thunderstorm activity in northeastern Colorado appears to have been lighter than usual during the summer of 1963. No measurements have been obtained to date on storms producing significant hail *at the ground*. As a result, this memorandum is limited to rather weak storms on three days during the month of June. On the basis of this analysis, which is described in detail in the following sections, these conclusions can be drawn:

(1) The precipitation scatter signals were observed on all three days, with the strongest being 15 db above the tropospheric scatter signal observed with the antennas directed at each other.

(2) Precipitation scatter signals were received on occasion from showers well outside the half-power points of the transmitter beam.

(3) Computed scattering cross sections for showers agree with those predicted on the basis of work with weather radar sets.

(4) There is definite evidence of Mie scattering at *X* band, with the departures from Rayleigh scattering being greatest near and above the freezing level. The most pronounced Mie effects are attributed to dry hailstones about 1.5 cm in diameter.

II GEOMETRY OF EXPERIMENT

The CRPL forward-scatter experiment uses low-gain transmitting antennas to illuminate entire showers or groups of showers with continuous-wave radiation, and scans the illuminated regions with very high-gain receiving antennas. For this situation, the beam geometry is rather simple (Fig. 1); theoretically, the common volume can be considered to include all of the receiver beam between the half-power points of the transmitter beam. Usually, however, the length of the contributing region (along the receiver beam) is restricted further by the dimensions of the shower causing the scattering. For such a case, Eq. (12) of Ref. 1 can be adapted to the form

$$P_r = \frac{P_t G_t}{4\pi R_t^2} \cdot \eta V \cdot \frac{G_r \lambda^2}{(4\pi R_r)^2} , \tag{1}$$

where P_r is the (mean) received power,

P_t is the transmitted power,

G_t is the gain of the transmitting antenna,

η is the scattering cross section per unit volume for scattering in the direction of the receiver, averaged over that part of the shower in the receiver beam,

V is the volume contributing to the received power,

G_r is the gain of the receiving antenna,

λ is the wavelength of the radiation,

R_t is the range of the shower from the transmitter, and

R_r is the range of the shower from the receiver.

Upon rearrangement, this yields

$$\eta V = \frac{(4\pi)^3 R_t^2 R_r^2 P_r}{\lambda^2 G_t G_r P_t} . \tag{2}$$

In the present case, we can write

$$V = L \cdot \frac{4\pi R_r^2}{G_r} , \tag{3}$$

where L is the length the shower extends along the receiver beam. Substitution of this in Eq. (2) leads to

$$\eta L = \frac{(4\pi)^2 R_t^2 \cdot P_r}{\lambda^2 G_t \cdot P_t} . \tag{4}$$

As η has dimensions of reciprocal length (area per unit volume), ηL is a pure number.

The equipment characteristics for the present experiment are shown in Table I.

The receiver beamwidths are approximately 15 minutes at X band and 30 minutes at C band. At a range of say, 100 km, the C-band receiver beam is only 0.9 km wide, well under the diameter of a typical shower. We can assume, therefore, that L is the same for the two frequencies, and use the following simple formula:

Table I

EQUIPMENT CHARACTERISTICS, CRPL SCATTER EXPERIMENT

	X BAND	C BAND
f (Gc)	9.10	4.86
λ (cm)	3.3	6.2
P_t (watts)	1000	1000
G_t (db)	22	25
G_r (db)	60	56

$$\frac{\eta_x}{\eta_c} = \frac{P_{rx} \lambda_c^2 G_{tc} P_{tc}}{P_{rc} \lambda_c^2 G_{tx} P_{tx}} \tag{5}$$

where all symbols are as defined previously, apart from the addition of the subscripts x and c. Substituting numerical values from Table I, we find

$$\frac{\eta_x}{\eta_c} = 10^{0.8} \frac{P_{rx}}{P_{rc}} . \tag{6}$$

The CRPL equipment operates in very narrow bands, 500 cps wide for the X-band system and 1,200 cps for the C-band. These are comparable

with the Doppler shifts associated with the motions of precipitation particles. As the combined elevation angles of the transmitter and receiver beams never exceeded 6°, the Doppler shift for storms off the direct path can be estimated from the horizontal wind, neglecting particle fall velocities and vertical currents. Let $\mathbf{s}_T$ and $\mathbf{s}_R$ be unit vectors directed from the shower toward the transmitter and receiver, respectively, and V be the wind vector in the part of the shower contributing to the scattered signal. Then the Doppler shift of the signal produced by a particle moving with the wind is given by

$$\Delta f = \frac{1}{\lambda}[\mathbf{s}_T \cdot \mathbf{V} + \mathbf{s}_R \cdot \mathbf{V}] \quad . \tag{7}$$

In some of the cases studied, the Δf computed for the X-band system was comparable to the 500-cps bandwidth, and so it is likely that some signal was lost occasionally through being shifted out of the receiver pass band. At C band, the shifts are smaller and the pass band wider; no cases were found where this effect would be serious.

The scatter signal produced by precipitation is incoherent, because the particles within the contributing region move with respect to one another. This leads to a broadening of the spectrum of the received signal, of the order of a few hundred cycles per second, in addition to the systematic Doppler shifts. The time to independence for rain and hail at X band and C band is a few milliseconds, being shorter at the higher frequency. The frequency response of the recording equipment used in the CRPL experiment is too low to show these fluctuations in full. The traces do fluctuate, but the signals as shown are smoothed to some extent.

III ANALYSIS OF DATA

A. GENERAL

The records chosen for analysis were obtained on 14, 26, and 27 June 1963. On 26 and 27 June, vertical polarization was used at the transmitters and receivers, so that, for scatterers off the Great Circle path, the scattered component perpendicular to the observation plane was recorded. Thus the scattered signals were contributed by the i_1 term of the Mie scattering theory.[4] For the special case of Rayleigh scattering ($\alpha = 2\pi\, a/\lambda \ll 1$, where a is the particle radius), i_1 is independent of the scattering angle, θ. On 14 June horizontal polarization was used, so that, for scatterers off the Great Circle path, the component parallel to the scattering plane was observed. The signals observed in this case are contributed by the i_2 term of the Mie theory, which vanishes for Rayleigh scatterers at $\theta = \pi/2$. However, most of the 14 June observations were made with θ near 30°, where i_2 is not much smaller than i_1.

On 26 and 27 June, some observations were made with the antennas directed toward each other in azimuth. In this case, the observation plane is vertical and the response is in the i_2 term, rather than the i_1 term. However, as i_1 and i_2 are defined relative to the observation plane, this switch merely serves to maintain the original polarization (vertical in this case).

The signals were analyzed as follows. The intersection of the transmitter and receiver beams was plotted to provide a first estimate of the location of the shower yielding the scattered signal. Because of the width of the transmitter beam, it was sometimes necessary to use the New Raymer radar data to fix the shower location and determine R_t and R_r accurately. By substituting for R_t and the observed power levels in Eq. (4), estimates of (ηL) were obtained for C band and X band, as all the other factors are constant. The height of the contributing region was computed from R_r and the elevation angle of the receiver beam. Upper wind data from Denver were used in estimating the Doppler shifts associated with horizontal particle motions. Finally, L was determined from time-lapse photographic records from the New Raymer radar, proper

allowance being made for the beam width of the radar set, permitting an estimate of the average value of η for that part of the shower in the receiver beam.

The strongest signals observed during the three days were −97 dbm at *X* band and −103 dbm at *C* band. On 27 June, some observations of the tropospheric scatter signal were made with the beams directed at each other; the observed signals averaged −113 dbm at *X* band and −118 dbm at *C* band. Thus, the precipitation scatter signals from the isolated showers ran as much as 15 db above the troposcatter signal on the direct path. The path was short (170 km) compared to many troposcatter links; as troposcatter signals decrease more rapidly with distance than do precipitation scatter signals, the excess of the precipitation scatter signal over the troposcatter signal would have been larger on a longer path.[1]

The tropospheric scatter signal, like the precipitation scatter, is incoherent, but with a time to independence of the order of a second, that is, comparable to the time lag in the recording apparatus, as compared with a few milliseconds for the precipitation scatter. Thus, the troposcatter signals undergo little averaging over time, so that *as recorded* they appear to fluctuate more widely than do the precipitation scatter signals.

B. A SITUATION IN DETAIL

Figure 2 shows in detail the situation at 1510 MST on 27 June. The three showers are shown as revealed by the New Raymer radar, after the beamwidth correction. The transmitter bearing was 240°; on the basis of the gains of the transmitting antennas, shown in Table I, the half-power bearings are estimated at 234° and 246° for the *C*-band beam and 232° and 248° for the *X*-band beam. The graph projection at lower right shows the power received with the receiver elevation angle at 0.5° as a function of receiver bearing, at both *X* band and *C* band. It is seen that quite strong signals were received at times when the only showers present in the receiver beam were outside the half-power points of the transmitter beam.

Thunderstorm tops are often elongated by wind shear, with ice crystals large enough to be detected by *X*-band radars carried many miles away from the storm cores. The New Raymer radar, operating on a low elevation angle, would show only the cores. However, the low elevation angle of the receiver beam in this case ensures that the scatter signals also originated

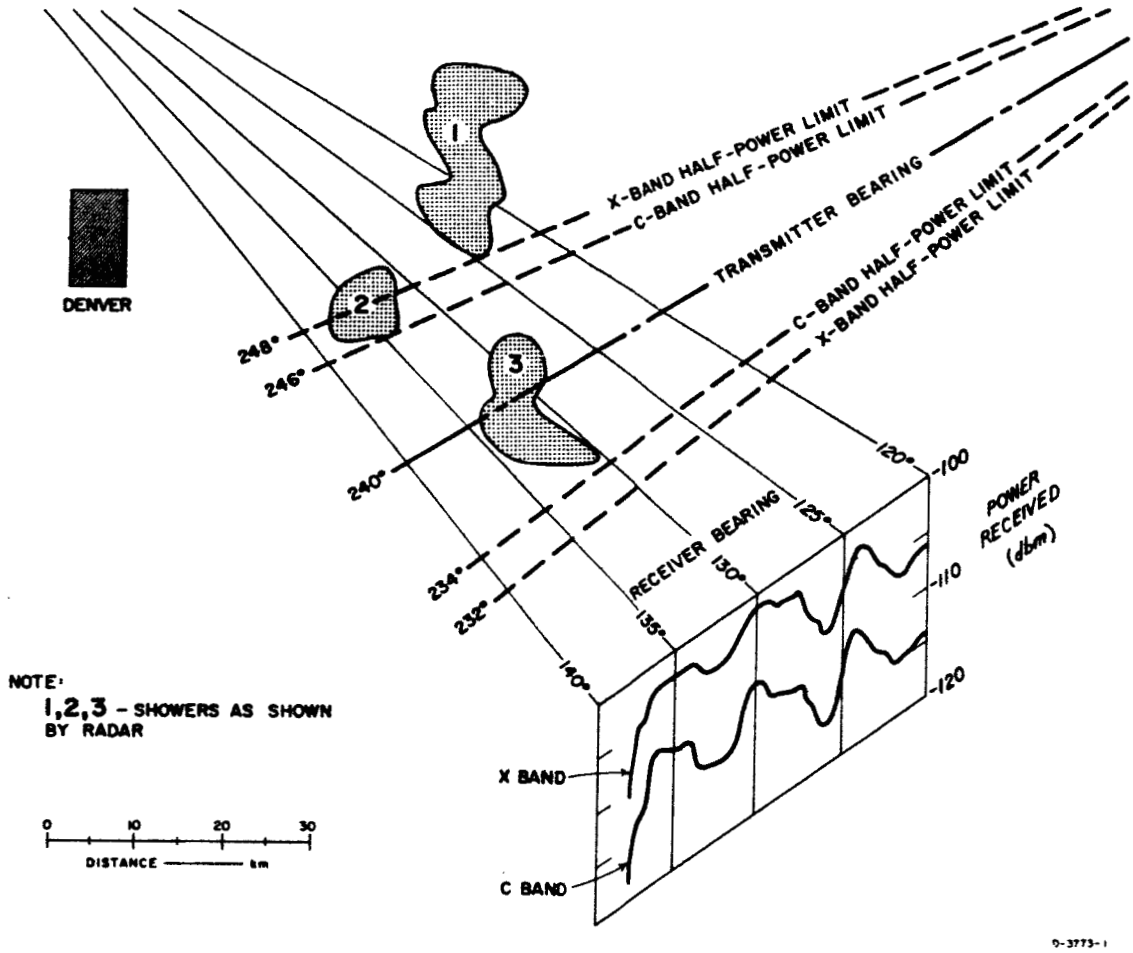

FIG. 2 SHOWER LOCATIONS AND RECEIVED POWER AS A FUNCTION OF RECEIVER BEARING, 1510 MST, 27 JUNE 1963

in the lower parts of the showers, within 2 km of the ground. Therefore, we conclude that the signals received on bearings of less than 126° are due entirely to Shower 1 and those received on bearings of more than 135° are due entirely to Shower 2. The signals received on bearings between 126° and 135° are due primarily to Shower 3, with some contributions from Shower 2. Shower 3 shows evidence of a multicellular structure on both the radar photographs and the forward scatter records. The receiver was not scanned through bearings less than 120°, so it is impossible to state what signals would have been received from the northern part of Shower 1.

The fact that detectable signals are received from showers outside the transmitter beam's half-power points indicates that reliable statistics on the scattering efficiency of showers cannot be obtained by reference to forward-scatter data only.

C. CALCULATIONS OF SCATTERING CROSS SECTIONS

The function (ηL) has been computed as described above for those cases where the radar data showed showers in the common volume of the transmitter and receiver beams. The maximum values, −26 db at X band and −43 db at C band, occurred in a shower observed at 1548 MST on 27 June, 90 km from the receiver site on a bearing of 117°. In this case, L was 6 km; hence η_x and η_c were −64 db m^{-1} and −81 db m^{-1}, respectively.

If one were to assume that the precipitation particles were Rayleigh scatterers, following previously observed typical raindrop-size distributions, one could deduce a rainfall rate of 4 mm/hr on the basis of the X-band observation, but only 2 mm/hr on the basis of the C-band observation (Fig. 1 of Ref. 2). This apparent discrepancy is due to the fact that non-Rayleigh scattering was taking place at the X-band frequency (see Sec. III-D).

The data studied contain 18 cases where it is possible to compute ηL and the average value of η with the receiver beam passing through the core of a precipitation cell. The geometric average of η_x, that is, the average of the individual cases expressed on a decibel scale, is 70 db m^{-1}; the geometric average of η_c over the 18 cases is −88 db m^{-1}.

The average value of η_c just quoted corresponds to a rainfall rate of the order of 0.5 mm/hr, which is quite low. However, there is a tendency for rainfall rates in showers to increase sharply with increasing penetration toward the center. Therefore, one would expect rainfall rates near the centers to exceed the computed values, which are averages along a diameter, by a considerable margin.

In analyzing the radar reflectivity within showers, Dennis has suggested the formula

$$Z' = C(r_0 - r)^{2.5} \quad , \tag{8}$$

where Z' is the equivalent reflectivity [Eq. (10) of Ref. 1],

C is a constant for a particular shower,

r_0 is the shower radius, and

r is distance measured from the shower center.[5]

In the case of Rayleigh scatterers, the equivalent reflectivity is simply the sum of the sixth powers of the particle diameters per unit volume. In all cases, it is related to $\eta(\pi)$, the *back-scattering* cross section per unit volume, by

$$Z' = (3.5 \times 10^{15}\lambda^4)\eta(\pi) \quad , \tag{9}$$

where Z' is expressed in $mm^6\ m^{-3}$, λ in meters, and $\eta(\pi)$ in reciprocal meters.

With r_0 and r expressed in kilometers, the parameter C in Eq. (8) ranges from around 4, in polar airmasses with dewpoints near 0°C, up to 100, in humid tropical air. The appropriate value for dry, summer conditions in Colorado is estimated at 10. Substitution of this in Eq. (8), integration along a shower diameter, and the use of Eq. (9), lead to the curves of Fig. 3. These show the expected maximum value of (ηL) as a function of shower radius at 4.86 and 9.10 Gc.

The X's and C's on Fig. 3 show the measured maximum values of $(\eta_x L)$ and $(\eta_c L)$ from the present study plotted against $L/2$, considered as the radius. The agreement with the curves based upon the model is quite good, especially at C band. It should be noted that, in the cases with non-Rayleigh scattering at X band, the back-scattering cross sections would be smaller than the observed forward-scatter cross sections, and so would agree somewhat better with the curve based upon the shower model.

D. EVIDENCE OF MIE SCATTERING

As the Rayleigh scattering cross section varies as f^4, the ratio η_x/η_c for Rayleigh scatterers in the present study is 11 db. The observed values of the ratio range from 10 to 25 db, so the ratio for Rayleigh scatterers serves as a lower bound, within the limits of measurement error. It is possible that the X-band signal was reduced on occasion by as much as 3 db by Doppler effects, but no attempt to correct for this effect is made in this section.

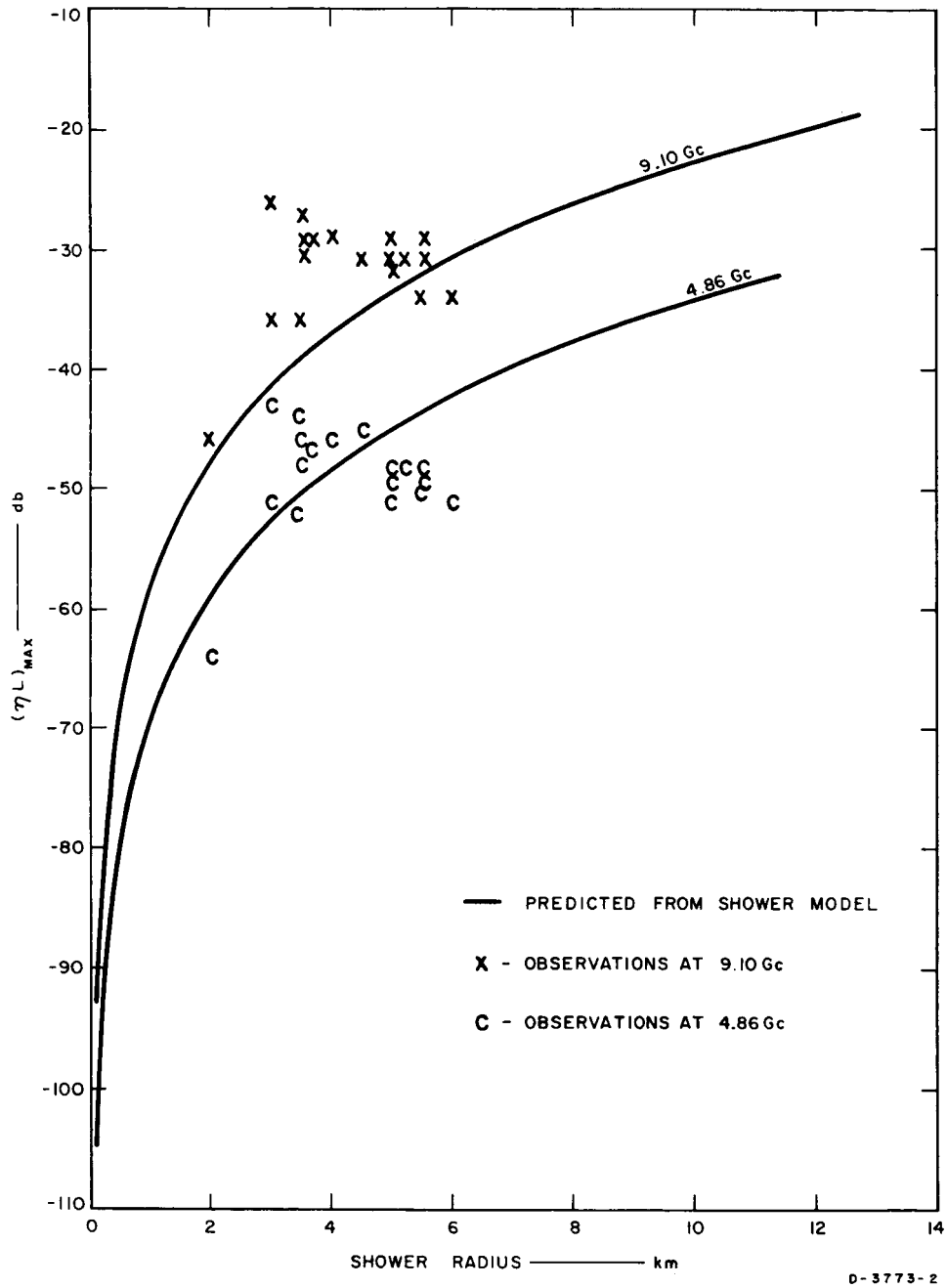

FIG. 3 INTEGRAL OF REFLECTIVITY ALONG SHOWER DIAMETER AS A FUNCTION OF SHOWER SIZE

Attempts have been made to correlate the ratio η_x/η_c with the scattering angle θ, with the height of the contributing region, and with η_c. The ratio does not show a significant correlation with any of the three parameters. As attenuation is more important at X band than at C band, the records have been examined to see if the low values of the ratio are associated with contributing regions shielded from the transmitter or receiver by intervening showers. No evidence of such an effect has been found, and the low *average* rainfall rates derived above indicate that attenuation is of minor importance in the small showers under consideration.

The variations in the ratio η_x/η_c are real and systematic, however. This is clearly seen in Fig. 4, which shows the measured ratio as a function of receiver bearing and elevation of the contributing region between 1607 and 1619 MST on 27 June. The reflectivity at C band in the same region is shown in Fig. 5; comparison of Figs. 4 and 5 shows that the maximum of η_x/η_c does not coincide with the shower core as shown by η_c. Of particular significance is the fact that the ratio is a maximum some 4 km above ground, whereas η_c reaches its maximum close to or at the ground.

The ratios shown in Fig. 4 can be explained logically on the basis of figures presented by Herman and Battan[4] and by Gunn and East.[6] Herman and Battan have computed the Mie scattering functions, $i_1(\theta)$ and $i_2(\theta)$, for ice spheres for various values of α (= $2\pi a/\lambda$) up to 5. Their results are computed for the wavelength 3.2 cm, but should be applicable at C band as well, since the refractive index of ice is independent of frequency in the microwave region.[6] Angular scattering functions for water drops in the microwave region are not available. However, it appears that the relative efficiency of scattering in a given direction at two different frequencies can be estimated from Fig. 6, which is reproduced from Gunn and East. This figure shows the ratio of Q_t (Mie), the total Mie cross section (scattering plus absorption), to Q_t (Rayleigh), the total Rayleigh cross section, for water drops at 18°C at several frequencies in the microwave region. Figure 9 of Ref. 4 shows that the fraction of the total scattering contained in the cones defined by $\theta < 10°$, $\theta < 20°$, and so on, is a slowly varying function of α. Therefore, we will make use of Fig. 6 in estimating the ratio η_x/η_c for raindrops.

From Fig. 6, it is found that the maximum possible η_x/η_c for raindrops occurs for drops of 3-to-4-mm diameter. In this range, the ratio

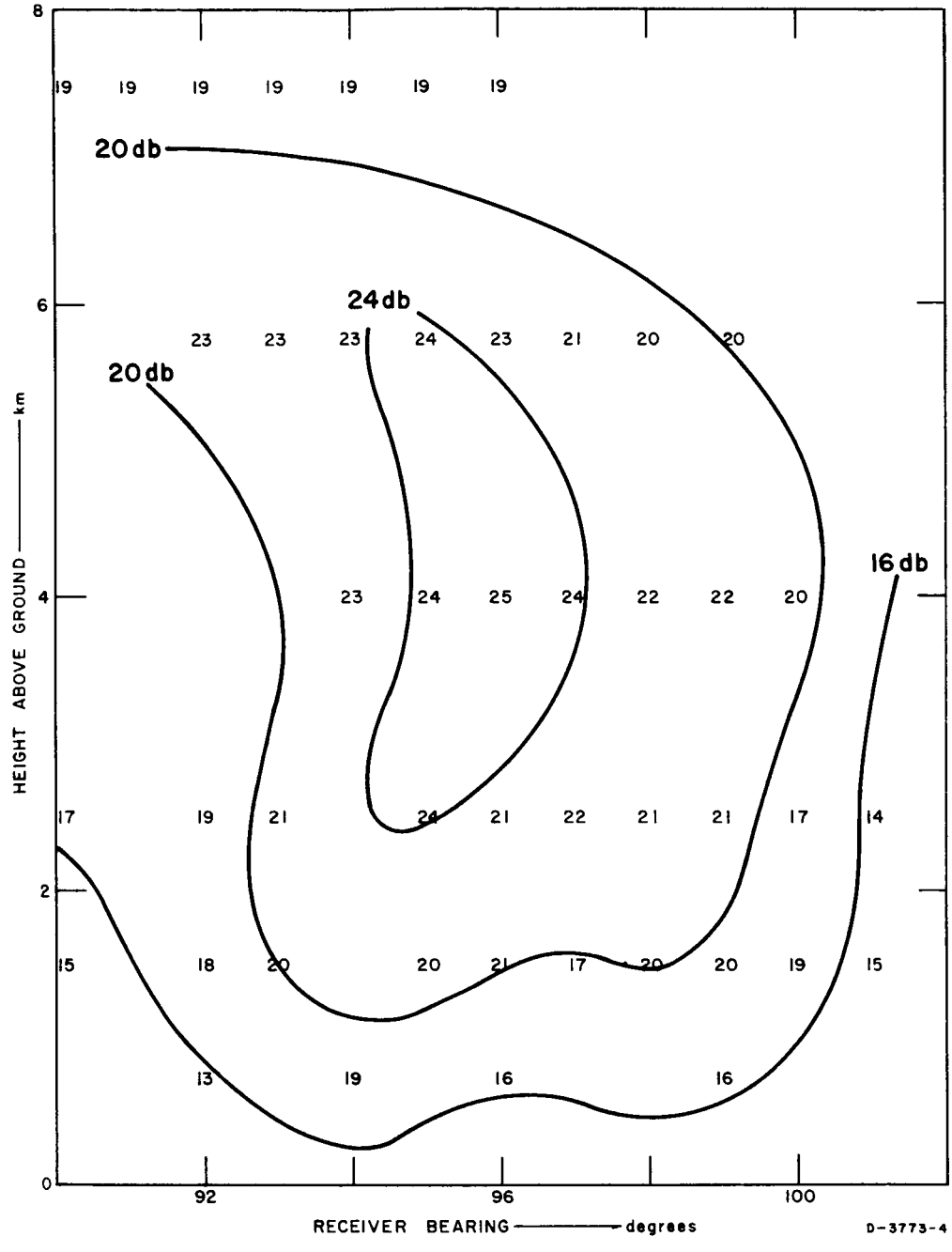

FIG. 4 RATIO OF OBSERVED SCATTERING CROSS SECTION AT 9.1 Gc TO THAT AT 4.86 Gc, 1607-1619 MST, 27 JUNE 1963

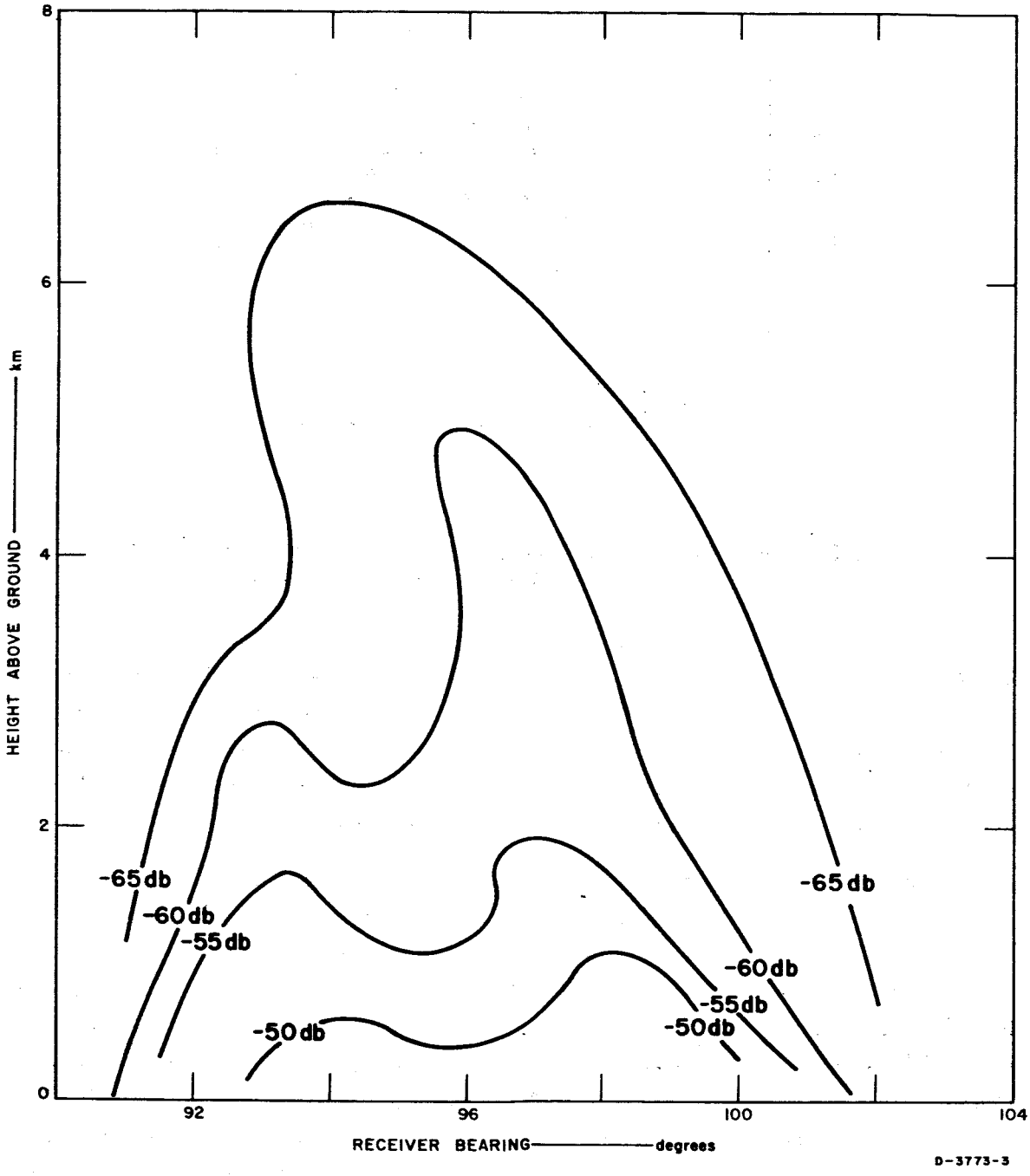

FIG. 5 MEASURED VALUES OF $\eta_c L$, 1607-1619 MST, 27 JUNE 1963

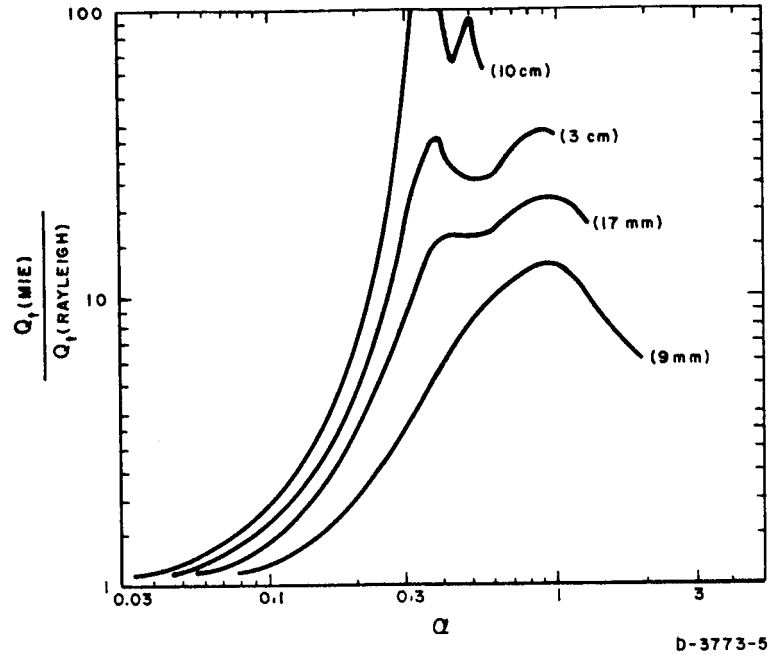

FIG. 6 RATIO OF ACTUAL ATTENUATION (by Scattering and Absorption) TO THAT GIVEN BY THE RAYLEIGH APPROXIMATION, FOR WATER AT 18°C

of Q_t (Mie) to Q_t (Rayleigh) is approximately 6 times (8 db) larger at 9.1 Gc than it is at 4.86 Gc. By adding in the 11 db difference for Rayleigh scatterers, it is found that η_x/η_c cannot exceed 19 or 20 db if the scatterers are raindrops or wet spherical hailstones, which have scattering properties resembling those of raindrops.

Herman and Battan's results on ice spheres show that the most rapid increase of forward-scattering cross sections with α occurs somewhere in the range $0.5 < \alpha < 1.5$. The function $i_1(\theta)$ for $\theta < 10°$ is about 32 db larger at $\alpha = 1.5$ than at $\alpha = 0.5$. This function must be weighted by λ^2 to obtain the scattering cross sections. In the present case, $(\lambda_c/\lambda_x)^2$ is near 5 db, leaving 27 db as the ratio of the forward-scattering cross sections at $\alpha = 1.5$ and $\alpha = 0.5$. In the present case, the ratio of α at X band to that at C band is near 2, rather than 3. Unfortunately, the functions for $\alpha = 1.0$ are not presented in Ref. 4; it appears likely, however, that the 27-db range is concentrated in the upper part of the range of α, rather than being uniformly distributed between 0.5 and 1.5. Therefore, it is most likely that the observed cases with η_x/η_c in excess of 20 db are due to dry hail with α near 1.5 at X band and 0.8 at C band,

that is, hail with the greater part of the signal contributed by stones near 15-mm diameter. This is consistent with the data of Fig. 5, where the maximum value of η_x/η_c is shown at 4 km above ground, well above the melting level. It is possible that shape effects play a part here also, but they cannot be assessed accurately as the Mie functions have not been generalized to large nonspherical particles. Studies of back-scattering by small ellipsoids show that significant effects could occur.

The decrease in η_x/η_c toward the top of the storm can be attributed to a preponderance of fine hailstones or snow crystals or both; the decrease in η_x/η_c downward from the 4-km level can be attributed to a preponderance of liquid water in the lower part of the shower. It is interesting to note the approach to Rayleigh scattering near the lower edges, where relatively small raindrops are ordinarily encountered. From Fig. 6, it would appear that drop diameters there are 1 to 2 mm. As small water drops are more efficient scatterers than ice spheres of the same size, the increase in reflectivity at *C* band with decreasing height can be attributed to the melting of hailstones to raindrops. The downward indentation of the −60-db contour on Fig. 5 coincides with the downward extension of the −24-db contour on Fig. 4; it may be associated with a shaft of falling hail, with the stones not showing appreciable melting until close to the ground.

ACKNOWLEDGMENTS

The authors wish to express their appreciation to those personnel of the Central Radio Propagation Laboratory, Colorado State University, Atmospherics, Inc., and the U.S. Weather Bureau, who assisted them by providing data used in the preparation of this memorandum.

REFERENCES

1. A. S. Dennis, "Forward Scatter from Precipitation as an Interference Source at Stations Monitoring Satellites," Research Memorandum 2 (Revised), Contract NASr-49-(02), SRI Project 3773, Stanford Research Institute, Menlo Park, California (November 1961).

2. A. S. Dennis, "Measurements of Forward Scatter from Rain at 9.05 Gc," Research Memorandum 4, Contract NASr-49-(02), SRI Project 3773, Stanford Research Institute, Menlo Park, California (May 1962).

3. L. H. Doherty and S. A. Stone, "Forward Scatter from Rain," *Trans. IRE, PGAP-8*, pp. 414-418 (July 1960).

4. B. M. Herman and L. J. Battan, "Calculations of the Total Attenuation and Angular Scatter of Ice Spheres," *Proc. Ninth Weather Radar Conference, Kansas City, Missouri, October 1961*, pp. 259-265 (American Meteorological Society, Boston, Massachusetts).

5. A. S. Dennis, "Rainfall Determinations by Meteorological Satellite Radar," Final Report, Contract NASr-49-(06), SRI Project 4080, pp. 47-53, Stanford Research Institute, Menlo Park, California (April 1963).

6. K. L. S. Gunn and T. W. R. East, "The Microwave Properties of Precipitation Particles," *Quart. J. Roy. Meteor. Soc.*, Vol. 80, pp. 522-545 (October 1954).

7. D. Atlas, M. Kerker, and W. Hitschfeld, "Scattering and Attenuation by Non-Spherical Atmospheric Particles," *J. Atmos. Terrest. Phys.*, Vol. 3, pp. 108-119 (February 1953).